

The first solution-processable n-type phthalocyaninato copper semiconductor: tuning the semiconducting nature *via* peripheral electron-withdrawing octyloxycarbonyl substituents[†]

Pan Ma,^{ab} Jinglan Kan,^a Yuexing Zhang,^a Chunhua Hang,^a Yongzhong Bian,^a Yanli Chen,^{*c} Nagao Kobayashi^d and Jianzhuang Jiang^{*a}

Received 4th July 2011, Accepted 19th September 2011

DOI: 10.1039/c1jm13082j

A series of unsymmetrical phthalocyaninato copper complexes simultaneously incorporating electron-withdrawing and electron-donating substituents at the phthalocyanine periphery Cu{Pc(15C5)}[(COOC₈H₁₇)₆] (**2**), Cu{Pc[adj-15C5]₂[(COOC₈H₁₇)₄]} (**3**), Cu{Pc[opp-15C5]₂[(COOC₈H₁₇)₄]} (**4**), Cu{Pc(15C5)₃[(COOC₈H₁₇)₂]} (**5**) were prepared and isolated. For comparative studies, symmetrical analogues including 2,3,9,10,16,17,24,25-octakis(octyloxycarbonyl)phthalocyaninato copper complex Cu[Pc(COOC₈H₁₇)₈] (**1**) and 2,3,9,10,16,17,24,25-tetrakis(15-crown-5)phthalocyaninato copper complex Cu[Pc(15C5)₄] (**6**) were also prepared. Their electrochemistry was studied by cyclic voltammetry (CV) and differential pulse voltammetry (DPV). With the help of a solution-based self-assembly process, these compounds were fabricated into organic field effect transistors (OFETs) with top contact configuration on hexamethyldisilazane (HMDS)-treated SiO₂/Si substrate. In line with the electrochemical investigation results, a p-type OFET with a carrier mobility (for holes) of 0.06 cm² V⁻¹ s⁻¹ was shown for Cu[Pc(15C5)₄] (**6**) with electron-donating 15-crown-5 as the sole type of peripheral substituent. In contrast, n-type devices with a carrier mobility (for electrons) of 6.7 × 10⁻⁶–1.6 × 10⁻⁴ cm² V⁻¹ s⁻¹ were achieved for **1–5** with electron-withdrawing octyloxycarbonyl substituents at the peripheral positions of phthalocyanine ring, indicating the significant effect of electron-withdrawing octyloxycarbonyl substituents on tuning the nature of phthalocyanine organic semiconductors. The present results represent the first example of solution-processed n-type phthalocyanine-based OFET devices.

Introduction

Organic field effect transistors (OFETs) with solution-processable organic semiconductors as active layers have attracted

significant research interest due to their great potential industrial applications in low-cost electronics including large area and flexible displays, active matrix electronic paper, simple smart cards and price tags.¹ Significant progress has been made in the past decade towards developing novel OFET materials such as conjugated polymers, oligomeric thiophenes, linear fused acenes, and perylenes with high carrier mobility, high ambient stability, and good solubility in common organic solvents.²

Metal phthalocyanines (MPcs) have been among the most promising active materials for OFETs due to their high thermal and chemical stability and good semiconducting properties.³ However, except for a few MPcs such as amino-(tri-*tert*-butyl) phthalocyaninato copper,⁴ hydroxydecyloxy-(tri-*tert*-butyl) phthalocyaninato copper,⁵ and sandwich-type bis/tris(phthalocyaninato) rare earth double/triple-decker complexes bearing long alkoxy substituents at the phthalocyanine peripheral positions that have been fabricated into OFETs through solution-based LB techniques,⁶ most efforts in this direction have been focused on the commercially available unsubstituted monomeric phthalocyanine compounds like MPc (M = Cu, Co, Fe, Mn, Ni, Zn).^{2a} Among these, CuPc is one of the most widely

^aDepartment of Chemistry, University of Science and Technology Beijing, Beijing, 100083, China. E-mail: jianzhuang@ustb.edu.cn; Fax: (+86) 10-6233-2462

^bDepartment of biology and Chemical Engineering, Luzhong Vocational College, Binzhou, 256200, China

^cSchool of Chemistry and Chemical Engineering, University of Jinan, Jinan, 250022, China. E-mail: chm_chenyl@ujn.edu.cn

^dGraduate School of Science, Tohoku University, Sendai, 980-8578, Japan

[†]Electronic supplementary information (ESI) available: Experimental and simulated isotopic patterns for molecular ion of phthalocyaninato copper complex **2**; Schematic representation of the unit cell in the aggregates of compounds **2–6** formed in methanol; IR spectra of complexes **1–6** in the region of 400–3100 cm⁻¹ with 2 cm⁻¹ resolution; Cyclic voltammogram of compounds **2** in CH₂Cl₂ containing 0.1M [NBu₄][ClO₄] at a scan rate of 20 mV S⁻¹; Drain–source current (*I*_{ds}) versus drain–source voltage (*V*_{ds}) characteristic at different gate voltage for the OFET of compound **2–5** on the HMDS-treated SiO₂/Si substrate; Electronic absorption data for the self-assemblies in methanol (**1–5**) or n-hexane (**6**). See DOI: 10.1039/c1jm13082j

used molecules for OFETs with hole transfer mobilities in the range of 10^{-5} – $1.0 \text{ cm}^2 \text{ V}^{-1} \text{ s}^{-1}$.^{3,7} Indeed, field effect transistors based on organic semiconductors are burgeoning with descriptions of hole transporting materials, which are the majority of OFET materials today. In contrast, electron-transporting n-type organic semiconductors have significantly lagged behind their p-type counterparts.⁸ Electron-transporting OFETs are important for the implementation of complementary circuits, which have low power consumption, high operating speeds, and an increased device lifetime. It has been revealed that for a material to transport electrons (n-channel), it needs to have an accessible lowest unoccupied molecular orbital (LUMO) level for electron injection and sufficient π -overlap to achieve reasonable charge carrier mobilities.⁹ Typically, CuPc-based n-type materials are made by attaching strong electron-withdrawing groups such as F,⁹ Cl,¹⁰ and CN¹¹ to the conjugated Pc core to lower the molecular orbital (MO) energy levels and allow electron injection by lowering the charge injection barrier. However, the unsubstituted or F, Cl, and CN-substituted phthalocyaninato copper complexes can only be fabricated into OFET devices by means of non-solution-based processes, such as vacuum deposition technique, due to their insolubility in common organic solvents. This actually retards their potential industrial applications in low price electronics. As a consequence, the design and synthesis of novel phthalocyaninato copper complexes, in particular for n-type semiconductors with solution-processability, still remains a challenge for phthalocyanine chemists and material scientists.

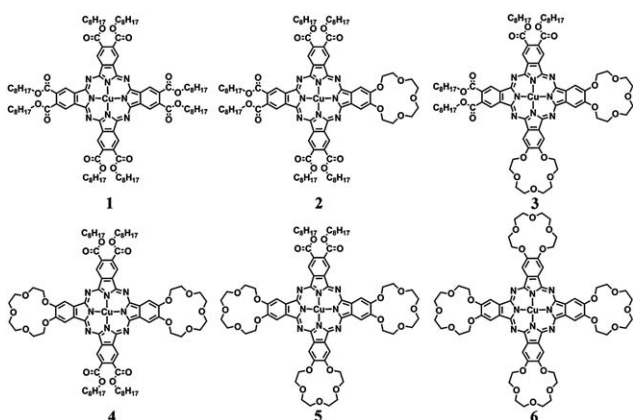
In the present paper, we describe the synthesis and electrochemical properties of a novel series of phthalocyaninato copper complexes $\text{Cu}[\text{Pc}(\text{COOC}_8\text{H}_{17})_8]$ (**1**), $\text{Cu}[\text{Pc}(15\text{C}5)(\text{COOC}_8\text{H}_{17})_6]$ (**2**), $\text{Cu}[\text{Pc}(\text{adj-}15\text{C}5)_2(\text{COOC}_8\text{H}_{17})_4]$ (**3**), $\text{Cu}[\text{Pc}(\text{opp-}15\text{C}5)_2(\text{COOC}_8\text{H}_{17})_4]$ (**4**), $\text{Cu}[\text{Pc}(15\text{C}5)_3(\text{COOC}_8\text{H}_{17})_2]$ (**5**), and $\text{Cu}[\text{Pc}(15\text{C}5)_4]$ (**6**) { $\text{Pc}(\text{COOC}_8\text{H}_{17})_8 = 2,3,9,10,16,17,24,25$ -Octakis(octyloxycarbonyl)phthalocyanine; $\text{Pc}(15\text{C}5)[(\text{COOC}_8\text{H}_{17})_6] =$ dianion of 2,3-(15-crown-5)-9,10,16,17,24,25-hexakis(octyloxycarbonyl)phthalocyanine; $\text{Pc}[(\text{adj-}15\text{C}5)_2][(\text{COOC}_8\text{H}_{17})_4] =$ dianion of 2,3,9,10-bis(15-crown-5)-16,17,24,25-tetrakis(octyloxycarbonyl)phthalocyanine; $\text{Pc}[(\text{opp-}15\text{C}5)_2][(\text{COOC}_8\text{H}_{17})_4] =$ dianion of 2,3,16,17-bis(15-crown-5)-9,10,24,25-tetrakis(octyloxycarbonyl)phthalocyanine; $\text{Pc}(15\text{C}5)_3[(\text{COOC}_8\text{H}_{17})_2] =$ dianion of 2,3,9,10,16,17-tris(15-crown-5)-24,25-bis(octyloxycarbonyl)phthalocyanine; Pc

$(15\text{C}5)_4 = 2,3,9,10,16,17,24,25$ -tetrakis(15-crown-5)phthalocyanine], Scheme 1. 15-crown-5 voids were introduced onto the phthalocyanine periphery to improve the solubility of the copper complexes in common organic solvents and thus enable solution processability for these intrinsic organic semiconductors. This is also true for the introduction of octyloxycarbonyl substituents. However, it is worth noting that incorporating octyloxycarbonyl chains with electron-withdrawing nature¹² onto the phthalocyanine periphery actually aims to tune the semiconducting nature of phthalocyaninato copper complexes from p-type to novel n-type ones. OFETs fabricated from $\text{Cu}[\text{Pc}(15\text{C}5)_4]$ (**6**) with electron-donating 15-crown-5 as the sole peripheral substituents were made, showing p-type nature with a carrier mobility (for holes) of $0.06 \text{ cm}^2 \text{ V}^{-1} \text{ s}^{-1}$, while those fabricated from **1–5** containing electron-withdrawing octyloxycarbonyl peripheral substituents displayed n-type properties with a carrier mobility (for electrons) of 6.7×10^{-6} – $1.6 \times 10^{-4} \text{ cm}^2 \text{ V}^{-1} \text{ s}^{-1}$, highlighting the significant effect of electron-withdrawing octyloxycarbonyl substituents on the nature of phthalocyanine organic semiconductors. The present work not only develops a new series of phthalocyaninato copper complexes as novel organic semiconductors but more importantly, to the best of our knowledge, represents the first example of n-type solution-processed phthalocyaninato copper-based OFET devices.

Results and discussion

Synthesis

2,3,9,10,16,17,24,25-Octakis(octyloxycarbonyl)phthalocyaninato copper complex compound $\text{Cu}[\text{Pc}(\text{COOC}_8\text{H}_{17})_8]$ (**1**) was synthesized according to a recently developed procedure.¹² For the purpose of comparative study, 2,3,9,10,16,17,24,25-tetrakis(15-crown-5)phthalocyaninato copper complex $\text{Cu}[\text{Pc}(15\text{C}5)_4]$ (**6**) was also prepared following published methods.¹³ Nevertheless, a series of unsymmetrical phthalocyaninato copper (ii) complexes $\text{Cu}\{\text{Pc}(15\text{C}5)[(\text{COOC}_8\text{H}_{17})_6]\}$ (**2**), $\text{Cu}\{\text{Pc}[(\text{adj-}15\text{C}5)_2][(\text{COOC}_8\text{H}_{17})_4]\}$ (**3**), $\text{Cu}\{\text{Pc}[(\text{opp-}15\text{C}5)_2][(\text{COOC}_8\text{H}_{17})_4]\}$ (**4**), $\text{Cu}\{\text{Pc}(15\text{C}5)_3[(\text{COOC}_8\text{H}_{17})_2]\}$ (**5**) have been successfully prepared and isolated by mixed cyclization of the two corresponding phthalonitriles, *i.e.* 4,5-dicyanobenzo-15-crown-5 and 4,5-di(octyloxycarbonyl)phthalonitrile, in the presence of $\text{Cu}(\text{acac})_2 \cdot \text{H}_2\text{O}$ in a solid state reaction at 250–260 °C. This renders it possible to investigate the effect of the number of electron-withdrawing groups introduced onto the phthalocyanine ring on tuning the semiconducting nature of phthalocyanine compounds. It is noteworthy, again, that purification of general phthalocyanine compounds has been a challenge for chemists in this field, not to mention the separation of a series of closely related isomeric phthalocyanines. Fortunately, in the present case, all the phthalocyaninato copper complexes including the two adjacent and opposite isomers $\text{Cu}\{\text{Pc}[(\text{adj-}15\text{C}5)_2][(\text{COOC}_8\text{H}_{17})_4]\}$ (**3**) and $\text{Cu}\{\text{Pc}[(\text{opp-}15\text{C}5)_2][(\text{COOC}_8\text{H}_{17})_4]\}$ (**4**) could be separated and purified by general silica gel column chromatography. It is worth noting that in line with our previous report on the synthesis and density functional theory calculations of a whole series of benzo-fused low symmetry metal-free tetraazaporphyrin and phthalocyanine analogues,¹⁴ the separation and in particular identification of the



Scheme 1 Schematic molecular structures of complexes **1–6**.

two adjacent and opposite isomers $\text{Cu}\{\text{Pc}[(\text{adj-15C5})_2][(\text{COOC}_8\text{H}_{17})_4]\}$ (**3**) and $\text{Cu}\{\text{Pc}[(\text{opp-15C5})_2][(\text{COOC}_8\text{H}_{17})_4]\}$ (**4**) are quite difficult due to their identical molecular weight and similar molecular structures. However, repeated column chromatography processes finally led to the isolation of two fractions with the first one being the oppositely substituted isomer **4**, due to its molecular polarity being relatively small compared to that of the adjacently substituted analogue, and the second one the adjacent isomer **3**. All the newly prepared phthalocyaninato copper complexes gave satisfactory elemental analysis results. The Matrix-assisted laser desorption/ionization time-of-flight (MALDI-TOF) spectra of all these compounds showed the molecular ion (M)⁺ signals with correct isotopic pattern. The isotopic pattern closely resembles the simulated one as exemplified by the spectrum of the compound **2** given in Fig. S1 (see ESI).[†] At the end of this section, it is worth noting that unsymmetrically substituted phthalocyanine derivatives as a whole series still remain very rare, limited to $\text{H}_2\{\text{Pc}[(\text{R})_{2n}(\text{OCH}_2\text{CH}_2\text{OCH}_2\text{CH}_2\text{OCH}_2\text{CH}_2\text{OCH}_3)_{8-2n}]\}^{15}$ and $\text{Cu}[\text{Pc}(\text{15C5})_n]^{13a}$ ($n = 1-3$), to the best of our knowledge. In particular, the present phthalocyaninato copper complexes represent a new series of unsymmetrical phthalocyanine derivatives simultaneously bringing electron-withdrawing octyloxycarbonyl chains and electron-donating 15-crown-5 voids.

Electronic absorption spectra

Electronic absorption spectra of the series of phthalocyaninato copper complexes **1-6** were recorded in chloroform. Fig. 1 shows the electronic absorption spectra of **1-6**. Symmetrically substituted compounds **1** and **6** display typical electronic absorption spectra for monomeric phthalocyaninato metal complexes with the Soret and Q bands at 350 and 684 nm for **1**

and 337 and 677 nm for **6**, respectively. However, unsymmetrically substituted phthalocyaninato copper complexes **2-5** have similar electronic absorption feature to zinc complexes of tetraazaporphyrin-phthalocyanine or phthalocyanine-naphthalocyanine analogues in terms of the appearance of electronic spectra.^{14,16} As can be seen, in addition to the general Soret band observed in the range of 342–348 nm for **2-5**, intense and split Q bands are observed at 674 and 696 nm for **2**, 666 and 710 nm for **3**, and 668 and 694 nm for **5**, while one unsplit Q band at 684 nm for **4**. The reason for the Q band splitting of complexes **2, 3, 5** is the symmetry decrease, compared to complexes **1, 4, 6**.

The electronic absorption spectra of the aggregates for these phthalocyaninato copper compounds **1-5** in methanol and **6** in n-hexane are also recorded and given in Fig. 1 and Table S1 (see ESI),[†] which are different from those of **1-6** in CHCl_3 solution. Obvious band broadening was observed due to the significant intermolecular interaction in the self-assembled nanostructures. In comparison with the chloroform solution spectrum, the phthalocyanine Soret band for the nanostructures of **1** is significantly red-shifted from 350 to 380 nm, and the Q absorptions also red-shift from 684 nm to 754 nm. On the basis of Kasha's exciton theory,¹⁷ red-shift of the main absorption bands of **1** upon aggregation in methanol implies that the phthalocyanine molecules are enforced to adopt the *J* aggregation mode in the nanostructures.

As shown in Fig. 1B, in comparison with the spectrum in chloroform solution, the phthalocyanine Soret absorption for the nanostructures of **2** red-shifts from 348 to 359 nm, while the Q bands blue-shift from 674 and 696 nm to 642 and 684 nm. Kasha's point-dipole model provides a rationale for the observed phenomenon. The extreme cases are represented by a head-to-tail arrangement of the dipoles, which results in a red-shifted absorption band (*J* aggregate), and a parallel arrangement of the dipoles (*H* aggregate) with a blue-shifted absorption band.¹⁷ The red and blue shifted bands observed in the present case for aggregates of **2** appear to represent an intermediate case that is conventionally thought of as a slipped cofacial stack with an "edge-on" configuration between adjacent Pc chromophores of **2** molecules.¹⁸ This phenomenon has also been observed previously for porphyrin¹⁹ and perylene aggregates²⁰ with a slipped cofacial oriented structure, where two transition moments interact in face-to-face and parallel orientation to give rise to blue and red shifts, respectively.

As shown in Fig. 1(C-F), the phthalocyanine Soret band for the nanostructures of **3-6** significantly blue-shifts from 344, 346, 342, and 337 nm in CHCl_3 to 337, 335, 334, and 333 nm. This is also true for the main Q absorptions of these four compounds upon aggregation. On the basis of Kasha's exciton theory, blue-shifts in the main absorption bands of **3-6** upon aggregation are typically a sign of the effective face-to-face $\pi-\pi$ interaction between phthalocyanine molecules, indicating the formation of *H* aggregate from these complexes.

IR spectral spectra

Vibrational spectroscopy has been proved a versatile technique for studying the intrinsic properties of phthalocyanine compounds.²¹ In the IR spectra of **1-6**, Fig. S2 (see ESI),[†] in addition to the absorption bands contributed from the central

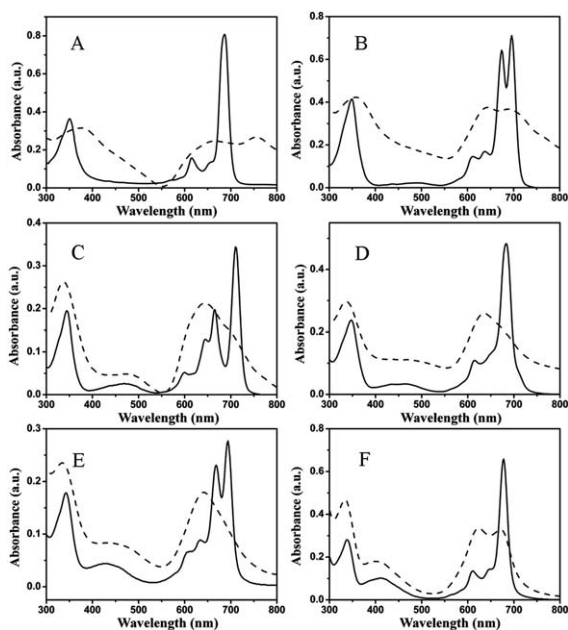


Fig. 1 Electronic absorption spectra of compounds **1-6** (A-F) in dilute chloroform solution (solid lines), nanostructures of compounds **1-5** (A-E) dispersed in methanol (dashed lines) and nanostructures of compound **6** (F) dispersed in n-hexane (dashed line).

aromatic Pc macrocycles including the wagging and torsion vibrations of C–H groups, isoindole ring stretching vibrations, and the C=N aza group stretching vibrations,²¹ the newly observed absorptions at 2845–2975, 1719–1729, 1271–1288, and 1081–1109 cm⁻¹ are attributed to the asymmetric and symmetric C–H stretching vibrations, C=O stretching vibrations, and asymmetric and symmetric C–O–C stretching vibrations of the octyloxycarbonyl and 15-crown-5 groups, respectively. The IR spectra of the self-assembled nano-structures of **1–6** are also shown in Fig. S2 (see ESI).[†] The similar feature in the IR spectra of the nano-structures to that of corresponding compounds for **1–6** unambiguously confirms that the nano-structures are composed of the corresponding phthalocyaninato copper compounds.

Electrochemical properties

The electrochemical behavior of the whole series of phthalocyaninato copper complexes **1–6** was investigated using cyclic voltammetry (CV) and differential pulse voltammetry (DPV) in CH₂Cl₂. These compounds display one one-electron oxidation labelled as Oxd₁ and two one-electron reduction (Red₁–Red₂) within the electrochemical window of CH₂Cl₂ under the present conditions. All these processes are attributed to successive removal from, or addition of one electron to, the ligand-based orbitals since the reduction of the central copper cation in these complexes does not occur in this range.²² The half-wave redox potential values vs. SCE (standard calomel electrode) are summarized in Table 1. Representative cyclic voltammograms for **2** are displayed in Fig. S3 (see ESI).[†]

As can be seen in Fig. S3 (see ESI)[†] and Table 1, the half-wave potentials of the first oxidation as well as the first and second reductions of these compounds correlate linearly with the number of the peripheral electron-withdrawing octyloxycarbonyl substituents, which are gradually shifted in the anodic direction along with the increase of the number of octyloxycarbonyl substituents from **6** to **1**, indicating that both of the HOMO and LUMO energy levels of the phthalocyaninato copper compounds get decreased along with the increase in the number of electron-withdrawing octyloxycarbonyl substituents. This result is in line with the experimental findings that the semiconducting nature of phthalocyaninato copper complexes changes from the p-type for **6** possessing peripheral electron-donating 15-crown-5 voids to n-type for **1–5** bearing peripheral electron-withdrawing octyloxycarbonyl substituents as detailed

Table 1 Half-wave redox potentials of **1–6** (*V* vs. SCE) in CH₂Cl₂ containing 0.1 M TBAP (Tetrabutylammonium perruthenate)

Compound	Oxd ₁	Red ₁	Red ₂	$\Delta E^{\circ}_{1/2}$ ^a	LUMO (eV)	HOMO (eV)
1 ^b	+1.14	-0.49	-0.81	1.65	-3.95	-5.58
2	+1.05	-0.59	-0.85	1.60	-3.85	-5.49
3	+0.92	-0.69	-0.90	1.61	-3.75	-5.36
4	+1.00	-0.79	-0.99	1.79	-3.65	-5.44
5	+0.88	-0.86	-1.07	1.74	-3.58	-5.32
6	+0.76	-1.02	-1.31	1.78	-3.42	-5.20

^a $\Delta E^{\circ}_{1/2}$ is the potential difference between the first oxidation and first reduction processes. ^b Cited from Ref. 12.

below. It is worth mentioning again that the unsubstituted analogue CuPc displays typical p-type semiconducting nature with good hole-carrier mobility.^{3,7}

The LUMO and HOMO energy levels can be estimated from the first reduction and oxidation potential (*vs.* SCE), respectively, on the basis of electrochemical results according to the literature method with the formula of $E_{\text{LUMO}} = -4.44 - E_{\text{Red}_1}$ and $E_{\text{HOMO}} = -4.44 - E_{\text{Oxd}_1}$, assuming that Koopmans' theorem holds.²³ On the basis of the first reduction and oxidation potentials revealed for compounds **1–6**, Table 1, LUMO energies of -3.95, -3.85, -3.75, -3.65, -3.58, and -3.42 eV are estimated for **1–6**, respectively, while the HOMO energy ranges from -5.58, -5.49, -5.36, -5.44, -5.32, to -5.20 eV for **1–6**. It is worth noting that to ensure the efficient electron injection from Au electrode with the work function of \sim -5.10 eV into the n-type organic semiconductor, a low-lying LUMO with the energy level less than -3.00 eV (*vs.* vacuum) is necessary.^{8a} Obviously, the estimated LUMO energy for all the six compounds **1–6** in the range of -3.95–-3.42 eV is smaller than -3.00 eV, indicating their potential n-type semiconductor nature. On the other hand, Marks and co-workers have reported that an empirical redox window between $E_{\text{Red}_1} = -0.4$ and 0.0 V (*vs.* SCE) is essential to achieve stable electron transport in air.²⁴ The LUMO energy of **1–6** still does not reach the range of air-stable n-type semiconductors with the LUMO energy lower than -4.04 eV (and in turn a first reduction potential more positive than -0.40 V *vs.* SCE) against the H₂O oxidation,²⁴ suggesting that the n-type semiconductor properties of these compounds might be detected only under an inert atmosphere. As detailed below, this is in line with the OFET properties shown for **1–5** in nitrogen. Nevertheless, the HOMO energy levels of **1–6** are just located within the range of -5.58–-5.20 eV, indicating their potential as p-type semiconductor materials.^{3,10} In particular, the HOMO level of **6** matches the work function of gold (-5.1 eV) very well, resulting in a low contact resistance and good ohmic hole injection from the source electrode into the semiconductor as verified below in the OFET property section.

X-ray diffraction patterns

The nanostructures of the series of complexes were fabricated by diffusion of methanol (**1–5**) or n-hexane (**6**) into the chloroform solution. The internal structure of self-assembled nanostructures of these complexes was investigated by XRD analysis, Fig. 2. As shown in Fig. 2A, in the low angle range, the XRD diagram of the aggregates formed from compound **1** shows three peaks at 2.56, 2.05, and 1.84 nm, respectively, which are ascribed to diffraction from the (100), (010), and (001) planes. In addition, the XRD pattern also displays four weaker higher order reflections at 1.03, 0.66, 0.51, and 0.42 nm, which are ascribed to diffraction from the (020), (030), (040), and (050) planes, revealing the high molecular ordering nature of this nanostructure along the *b*-axis of the unit cell. The (001) plane gives its higher order diffractions at 0.90 (002) and 0.60 (003) nm, and the (100) plane gives its higher order diffractions at 1.41 (200) and 0.69 (300) nm in the wide angle range of XRD pattern. These diffraction results could be assigned to refraction from a rectangular lattice with the cell parameter of $a = 2.56$ nm, $b = 2.05$ nm, and $c = 1.84$ nm, Fig. 3. It is worth noting that in the wide angle

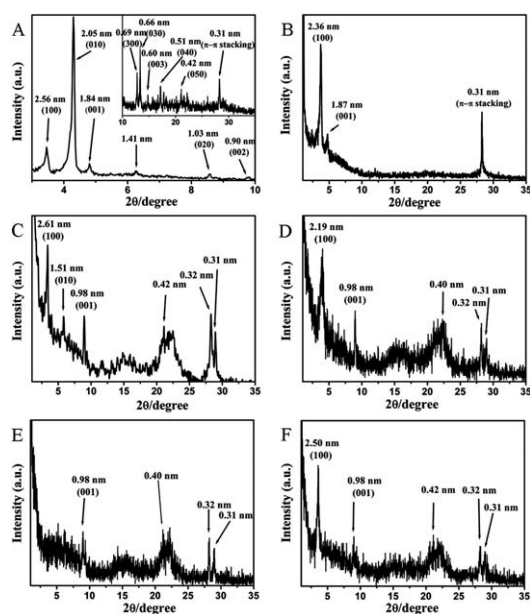


Fig. 2 XRD profiles of the aggregates of compounds 1–6 (A–F).

region, the nanowire XRD pattern of this compound shows additional refraction at 0.31 nm, which is attributed to the stacking distance between tetrapyrrole cores of neighboring phthalocyanine molecules along the direction perpendicular to the tetrapyrrole rings.²⁵

As shown in Fig. 2B, the XRD diagram of the aggregates formed from compound 2 shows two well-defined peaks at 2.36 and 1.87 nm, respectively, originating from the (100) and (001)

planes. These diffraction results could be assigned to refraction from a rectangular lattice with cell parameters of $a = 2.36$ nm and $c = 1.87$ nm, Fig. S4 (see ESI).[†] In the wide angle region, the peak at 0.31 nm is also observed, just the same as that observed for the nanostructures of compound 1.

As shown in Fig. 2C, the XRD diagram of the aggregates formed from compound 3 shows three well-defined peaks at 2.61, 1.51, and 0.98 nm, respectively, originating from the (100), (010), and (001) planes. These diffraction results could be assigned to refraction from a rectangular lattice with the cell parameters of $a = 2.61$ nm, $b = 1.51$ nm, and $c = 0.98$ nm, Fig. S5 (see ESI).[†] In addition, the XRD pattern displays a well-defined peak at the wide angle region corresponding to the distances of 0.42 nm that relates to the liquid-like order of the alkyl chains.²⁶ It is worth noting that in the wide angle region, the XRD pattern also presents two sharp refractions at 0.31 and 0.32 nm, respectively, associated with the π - π stacking of neighboring monomeric molecules in the dimer of the unit cell in the aggregates and neighboring dimers along the direction perpendicular to the phthalocyanine rings.²⁷

The XRD patterns of self-assembled nanostructures of 4, 5, and 6 show a weak peak at 0.98 nm, originating from the (001) plane, Fig. 2(D–F). Another refraction observed in the XRD patterns of the self-assembled nanostructures of 4 and 6 appears at 2.19 and 2.50 nm, respectively, which is ascribed to the refraction from the (100) plane, Fig. S6 (see ESI).[†] In the wide angle region, the peaks at 0.42, 0.40, 0.32, and 0.31 nm are also observed, just the same as those observed for the nanostructures of compounds 1, 2, and 3.

Morphology of the aggregates

The morphology of the aggregates formed from 1–6 was examined by scanning electron microscopy (SEM) and transmission electronic microscopy (TEM). Samples were prepared by casting a drop of sample solution onto a carbon-coated grid or SiO₂ substrate. The SEM and TEM images of aggregates of 1–6 are shown in Fig. 4 and 5, respectively. As shown in Fig. 4A and 5A, depending mainly on the head-to-tail inter-molecular π - π interactions in cooperation with the van der Waals interactions, compound 1 self-assembles into one-dimensional (1D) nanostructures with long, straight wire morphology several centimetres in length and about 500 nm–5 μ m in width. In combination with the electronic absorption and XRD analysis results, it could be proposed that the wire-like object is formed by the phthalocyanine disks in a “side-by-side” arrangement along the a -axis, which constructs the longitudinal direction of the wires, Fig. 3.

Compound 2 self-assembles into helical nanowires hundreds of microns in length and about 100 nm–3 μ m in width, Fig. 4B and 5B. Schematic illustration for the formation of helical nanowires is shown in Fig. S4 (see ESI)[†] on the basis of the XRD analysis as detailed above. As can be seen in this figure, four phthalocyanine molecules as building blocks stack into helical nanowires depending on inter-molecular π - π interactions in cooperation with the van der Waals interactions.

As displayed in Fig. 4C and 5C, depending mainly on the cofacial π - π interactions, compound 3 self-assembles into nanowires hundreds of microns in length and 100 nm–1 μ m in

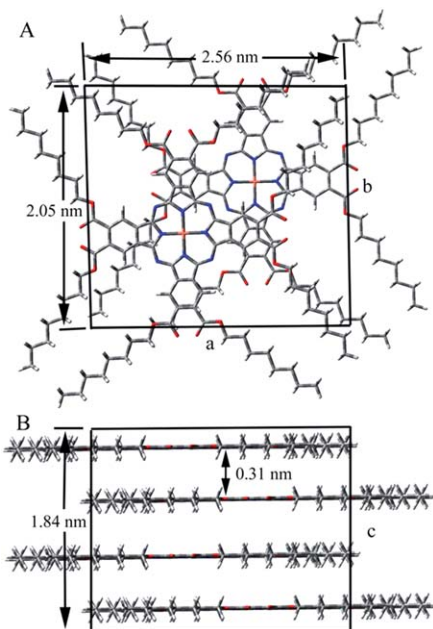


Fig. 3 Schematic representation of the unit cell in the aggregates of compound 1 formed in methanol: (A) top view and (B) side view. Hydrogen atoms are omitted for clarity. The blue lines indicate N atoms. The pink stands for the copper atom while the red part is the oxygen atom.

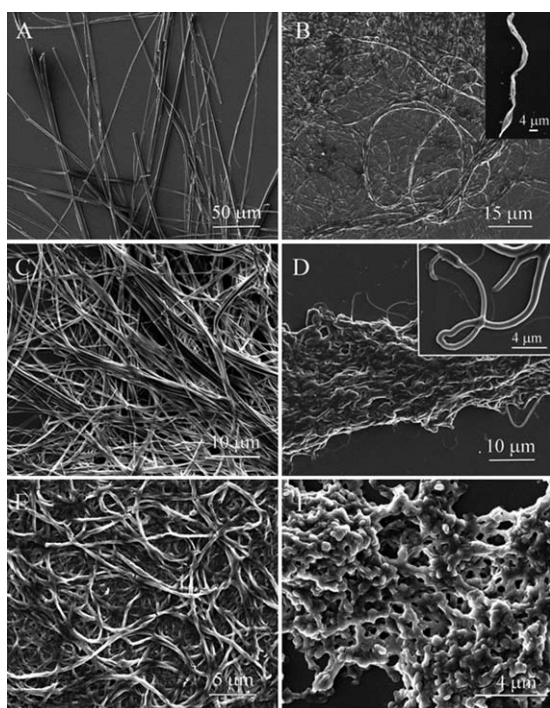


Fig. 4 SEM images of nanostructures of compounds 1–6 (A–E). The insets are is single nanowires of the corresponding compounds.

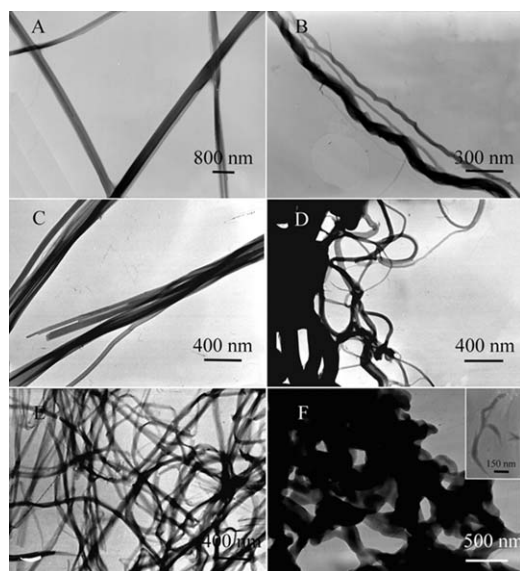


Fig. 5 TEM images of nanostructures of compounds 1–6 (A–E). The inset is a single nanofibril of compound 6.

width. Compounds 4 and 5 self-assemble into long, flexible one-dimensional (1D) nanowires hundreds of microns in length and 100–800 nm in width, while compound 6 self-assembles into one-dimensional (1D) nanostructures with wire bundle morphology several micrometres in length and 100–200 nm in width. The nanostructures are composed of several single fibrils. In combination with the electronic absorption and XRD analysis results, the nanowire objects are considered to be formed by the phthalocyanine dimeric building blocks in

a “face-to-face” arrangement along the *c*-axis, constructing the longitudinal direction of the nanowires, Fig. S5 and Fig. S6 (see ESI).†

OFET properties

The devices fabricated from the aggregates of 1–5 with top contact configuration show typical n-channel characteristics, while that from the aggregates of 6 displays typical p-channel characteristics, Fig. 6 and Fig. S7 (see ESI).† The carrier mobility (μ) was calculated by using the saturation region transistor equation, $I_{ds} = (W/2L)\mu C_0 (V_G - V_T)^2$, where I_{ds} is the source–drain current, V_G the gate voltage, C_0 the capacitance per unit area of the dielectric layer, and V_T the threshold voltage.²⁸ The devices fabricated from nanostructures of compound 1 on HMDS treated SiO₂/Si substrate have a carrier mobility (for electrons) of $1.6 \times 10^{-4} \text{ cm}^2 \text{ V}^{-1} \text{ s}^{-1}$ with an on/off ratio of 10^2 and a threshold voltage of -8 V , Fig. 6. In line with the increase of the LUMO energy level of 2–5 in comparison with 1 revealed by the electrochemical measurement, the carrier mobility (for electrons) for 2–5 decreases to 1.6×10^{-5} , 6.7×10^{-6} , 8.5×10^{-6} , and $1.2 \times 10^{-5} \text{ cm}^2 \text{ V}^{-1} \text{ s}^{-1}$, respectively, with the on/off ratio staying at 10^2 and the threshold voltage being about -3 , -7 , -5 , and -4 V . In good contrast, the device fabricated from nanostructures of 6 on a HMDS treated SiO₂/Si substrate has a carrier mobility (for holes) of $0.06 \text{ cm}^2 \text{ V}^{-1} \text{ s}^{-1}$ with an on/off ratio of 10^3 and a threshold voltage of -8 V . This is in line with the electrochemical measurement results as detailed above.

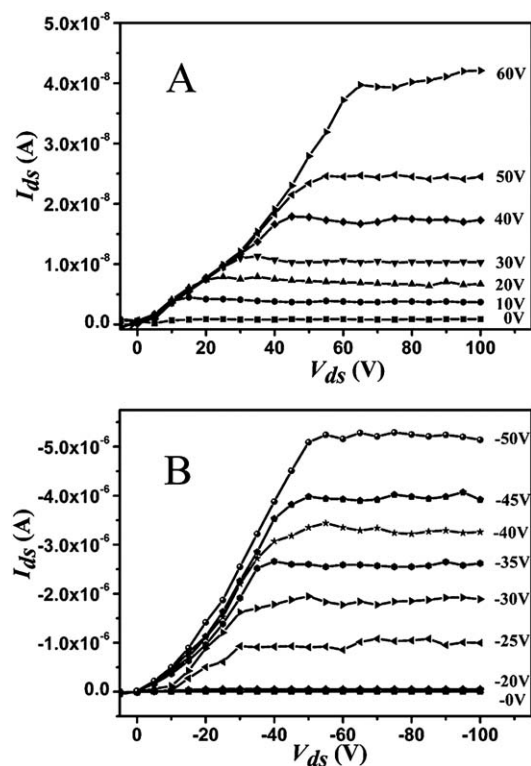


Fig. 6 Drain–source current (I_{ds}) versus drain–source voltage (V_{ds}) characteristics at different gate voltages for the OFET of compound 1 (A) and 6 (B) on the HMDS-treated SiO₂/Si substrate.

Conclusion

In summary, a series of six phthalocyaninato copper complexes with different numbers of peripheral electron-withdrawing octyloxycarbonyl and electron-donating 15-crown-5 substituents have been designed and prepared. These compounds have been fabricated into OFET devices by means of a solution-based self-assembly process and their performance was comparatively investigated. A p-type OFET device with carrier mobility for holes was fabricated from the compound with electron-donating 15-crown-5 as the sole type of peripheral substituents, while n-type devices with carrier mobility for electrons were fabricated from all the remaining compounds with peripheral electron-withdrawing octyloxycarbonyl substituents, indicating the significant effect of electron-withdrawing octyloxycarbonyl substituents on tuning the nature of organic semiconductors. The present result not only represents the first example of n-type solution-processed phthalocyaninato copper-based OFET devices, but more importantly sheds light on designing and preparing novel n-type solution-processable phthalocyanine semiconductors with good OFET performance.

Experimental section

Chemicals

Hexamethyldisilazane (HMDS) was purchased from Aldrich. Dichloromethane for voltammetric studies was freshly distilled from CaH_2 under nitrogen. Column chromatography was carried out on silica gel (Merck, Kieselgel 60, 70–230 mesh) with the indicated eluents. The electrolyte $[\text{Bu}_4\text{N}][\text{ClO}_4]$ was recrystallized twice from tetrahydrofuran. All other reagents and solvents were used as received. The compounds of 4,5-dicyanobenzo-15-crown-5, 4,5-di(octyloxycarbonyl)phthalonitrile, $\text{Cu}[\text{Pc}(\text{COOC}_8\text{H}_{17})_8]$ (**1**), and $\text{Cu}[\text{Pc}(15\text{C}_5)_4]$ (**6**) were prepared according to published procedures.^{12,13}

Measurements

Electronic absorption spectra were recorded on a Hitachi U-4100 spectrophotometer. IR spectra were recorded as KBr pellets using a Bio-Rad FTS-165 spectrometer with 2 cm^{-1} resolution. X-ray diffraction experiments were carried out on a Rigaku D/max- γ B X-ray diffractometer. MALDI-TOF mass spectra were taken on a Bruker BIFLEX III ultra-high resolution Fourier transform ion cyclotron resonance (FT-ICR) mass spectrometer with α -cyano-4-hydroxycinnamic acid as the matrix. Elemental analysis was performed on an Elementar Vavio El III. TEM images were measured on a JEOL-100CX II electron microscope operated at 100 KV. For TEM imaging, a drop of sample solution was cast onto a carbon copper grid. SEM images were obtained using a JEOL JSM-6700F field-emission scanning electron microscope. For SEM imaging, Au (1–2 nm) was sputtered onto the grids to prevent charging effects and to improve the image clarity. Substrates used in the present study were successively cleaned with pure water, acetone, and ethanol. Electrochemical measurements were carried out with a BAS CV-50W voltammetric analyzer. The cell comprised inlets for a glassy carbon disk working electrode of 2.0 mm in diameter and a silver wire counter electrode. The reference electrode was

Ag/Ag^+ (a solution of 0.01M AgNO_3 and 0.1M TBAP in acetonitrile), which was connected to the solution by a Luggin capillary whose tip was placed close to the working electrode. It was corrected for junction potentials by being referenced internally to the ferrocenium/ferrocene (Fe^+/Fe) couple. Typically, a 0.1 M solution of $[\text{NBu}_4][\text{ClO}_4]$ in CH_2Cl_2 containing 0.5 M of sample was purged with nitrogen for 10 min, and then the voltammograms were recorded at ambient temperature. The scan rates were 20 and 10 mV s^{-1} for CV and DPV, respectively.

OFET device fabrication

The heavily n-doped silicon layer functioning as the gate electrode. The nanostructures of the complexes **1–6** (1 mM) were fabricated in a binary solvent of chloroform : methanol (1 : 3) or chloroform : n-hexane (1 : 3) in a vial, which was left still for about 1 day. Then a drop of the nanostructure sample solution was cast onto a SiO_2 substrate. After the solution evaporated, the source–drain electrodes were thermally evaporated onto the aggregates by use of a shadow mask. These electrodes have width (W) of 28.6 nm and channel length (L) of 0.24 mm. The oxide layer of 5000 Å is the gate dielectric having a capacitance per unit area of 10 nF cm^{-2} . Before depositing the aggregates, surface treatment for SiO_2/Si substrates was performed according to literature method using HMDS, as detailed below.²⁹ OFET devices for compounds **1–5** were measured in a dry nitrogen glove box, and for **6** were measured in air. The current–voltage characteristics were obtained with a Hewlett-Packard (HP) 4140B parameter analyzer at room temperature.

A drop of HMDS was added to the cell culture dish (90 mm), which contained cleaned SiO_2/Si substrates. Then the cell culture dish was put into an airtight vial over night. After being taken out, the substrates were rinsed with chloroform and methanol, respectively, to remove the redundant HMDS.

Synthesis of unsymmetrical phthalocyaninato copper complexes 2–5

The mixture of dicyanobenzo-15-crown-5 (213 mg, 0.67 mmol), 4,5-di(alkoxy carbonyl)phthalonitrile (295 mg, 0.67 mmol), and $\text{Cu}(\text{acac})_2 \cdot \text{H}_2\text{O}$ (69 mg, 0.35 mmol) sealed under N_2 atmosphere was fused at *ca.* 250–260 °C for 20–30 min. After being cooled, the residue was washed well with water and methanol, and subjected to chromatography on a silica gel column (40 × 150 mm). Compound **1** was removed as the first fraction with CHCl_3 as the eluent. Then the column was eluted with a mixed solvent of CHCl_3 : triethylamine : CH_3OH to develop four successive fractions containing mainly the compound of **2**, **4**, **3**, and **5**, respectively, with gradually increasing the content of CH_3OH in the eluent from the ratio of 100 : 1 : 0.5, 100 : 1 : 2, 100 : 1 : 3, to 100 : 1 : 4 (v/v). The crude products were further purified by silica gel column chromatography (26 × 80 mm) with the above mentioned mixed solvent as the eluent. Recrystallization from CHCl_3 and methanol gave pure target compounds $\text{Cu}[\text{Pc}(15\text{C}_5)(\text{COOC}_8\text{H}_{17})_6]$ (**2**) as a blue powder and $\text{Cu}[\text{Pc}(\text{adj}-15\text{C}_5)_2(\text{COOC}_8\text{H}_{17})_4]$ (**3**), $\text{Cu}[\text{Pc}(\text{opp}-15\text{C}_5)_2(\text{COOC}_8\text{H}_{17})_4]$ (**4**), $\text{Cu}[\text{Pc}(15\text{C}_5)_3(\text{COOC}_8\text{H}_{17})_2]$ (**5**) as green powder.

$\text{Cu}[\text{Pc}(15\text{C}_5)(\text{COOC}_8\text{H}_{17})_6]$ (**2**) (46 mg, 8.3%). MS (MALDI-TOF) an isotopic cluster peaking at m/z 1703.6 (calc. for

M⁺ 1703.6). Anal. Calc. for CuC₉₄H₁₂₆N₈O₁₇: C, 66.27%; H, 7.45%; N, 6.58%. Found: C, 66.23%; H, 7.32%; N, 6.39%. UV-Vis (CHCl₃) [λ_{\max} nm (log ϵ)] 348 (4.94), 612 (4.49), 638 (4.56), 674 (5.14), 696 (5.18).

Cu[Pc(adj-15C5)₂(COOC₈H₁₇)₄] (3) (7 mg, 1.3%) MS (MALDI-TOF) an isotopic cluster peaking at *m/z* 1580.8 (calc. for [MH]⁺ 1580.3). Anal. Calc. for CuC₈₄H₁₀₆N₈O₁₈: C, 63.80%; H, 6.88%; N, 7.09%. Found: C, 63.73%; H, 6.52%; N, 6.83%. UV-Vis (CHCl₃) [λ_{\max} nm (log ϵ)] 344 (5.06), 600 (4.53), 646 (4.90), 666 (5.04), 710 (5.22).

Cu[Pc(opp-15C5)₂(COOC₈H₁₇)₄] (4) (45 mg, 8.1%) MS (MALDI-TOF) an isotopic cluster peaking at *m/z* 1580.5 (calc. for [MH]⁺ 1580.3). Anal. Calc. for CuC₈₄H₁₀₆N₈O₁₈: C, 63.80%; H, 6.88%; N, 7.09%. Found: C, 63.20%; H, 6.50%; N, 6.73%. UV-Vis (CHCl₃) [λ_{\max} nm (log ϵ)] 346 (4.91), 616 (4.59), 684 (5.17).

Cu[Pc(15C5)₃(COOC₈H₁₇)₂] (5) (20 mg, 3.7%) MS (MALDI-TOF) an isotopic cluster peaking at *m/z* 1460.1 (calc. for [MH]⁺ 1460.1). Anal. Calc. for CuC₇₄H₉₀N₈O₁₉: C, 60.91%; H, 6.22%; N, 7.68%. Found: C, 60.63%; H, 6.24%; N, 7.39%. UV-Vis (CHCl₃) [λ_{\max} nm (log ϵ)] 342 (4.74), 608 (4.35), 634 (4.50), 668 (4.81), 694 (4.83).

Acknowledgements

Financial support from the Natural Science Foundation of China, Beijing Municipal Commission of Education, and University of Science and Technology Beijing is gratefully acknowledged.

Notes and references

- (a) A. Tsumura, H. Koezuka and T. Ando, *Appl. Phys. Lett.*, 1986, **49**, 1210; (b) C. D. Dimitrakopoulos and P. R. L. Malenfant, *Adv. Mater.*, 2002, **14**, 99; (c) G. Horowitz, *Adv. Mater.*, 1998, **10**, 365.
- (a) W. Wu, Y. Liu and D. Zhu, *Chem. Soc. Rev.*, 2010, **39**, 1489; (b) R. P. Ortiz, A. Facchetti and T. J. Marks, *Chem. Rev.*, 2010, **110**, 205.
- (a) Y. Zhang, X. Cai, Y. Bian and J. Jiang, *Struct. Bond.*, in *Functional Phthalocyanine Molecular Materials*, ed. J. Jiang, Springer Press, 2010, **135**, 275; (b) Y. Sun, Y. Liu and D. Zhu, *J. Mater. Chem.*, 2005, **15**, 53.
- W. Hu, Y. Liu, Y. Xu, S. Liu, S. Zhou and D. Zhu, *Synth. Met.*, 1999, **104**, 19.
- K. Xiao, Y. Liu, X. Huang, Y. Xu, G. Yu and D. Zhu, *J. Phys. Chem. B*, 2003, **107**, 9226.
- (a) Y. Chen, W. Su, M. Bai, J. Jiang, X. Li, Y. Liu, L. Wang and S. Wang, *J. Am. Chem. Soc.*, 2005, **127**, 15700; (b) W. Su, J. Jiang, K. Xiao, Y. Chen, Q. Zhao, G. Yu and Y. Liu, *Langmuir*, 2005, **21**, 6527; (c) R. Li, P. Ma, S. Dong, X. Zhang, Y. Chen, X. Li and J. Jiang, *Inorg. Chem.*, 2007, **46**, 11397; (d) Y. Chen, R. Li, R. Wang, P. Ma, S. Dong, Y. Gao, X. Li and J. Jiang, *Langmuir*, 2007, **23**, 12549; (e) Y. Gao, P. Ma, Y. Chen, Y. Zhang, Y. Bian, X. Li, J. Jiang and C. Ma, *Inorg. Chem.*, 2009, **48**, 45.
- (a) Z. Bao, A. J. Lovinger and A. Dodabalapur, *Appl. Phys. Lett.*, 1996, **69**, 3066; (b) K. Xiao, Y. Liu, G. Yu and D. Zhu, *Appl. Phys. A: Mater. Sci. Process.*, 2003, **77**, 367; (c) K. Xiao, Y. Liu, G. Yu and D. Zhu, *Synth. Met.*, 2003, **137**, 991; (d) J. Yuan, J. Zhang, J. Wang, X. Yan, D. Yan and W. Xu, *Appl. Phys. Lett.*, 2003, **82**, 3967; (e) J. Wang, X. Yan, Y. Xu, J. Zhang and D. Yan, *Appl. Phys. Lett.*, 2004, **85**, 5424; (f) K. Xiao, Y. Liu, Y. Guo, G. Yu, L. Wan and D. Zhu, *Appl. Phys. A: Mater. Sci. Process.*, 2005, **80**, 1541; (g) X. Yan, H. Wang and D. Yan, *Thin Solid Films*, 2006, **515**, 2655; (h) Z. Bao, A. J. Lovinger and A. Dodabalapur, *Adv. Mater.*, 1997, **9**, 42; (i) R. Zeis, T. Siegrist and Ch. Kloc, *Appl. Phys. Lett.*, 2005, **86**, 22103; (j) Q. Tang, H. Li, M. He, W. Hu, C. Liu, K. Chen, C. Wang, Y. Liu and D. Zhu, *Adv. Mater.*, 2006, **18**, 65.
- (a) C. R. Newman, C. D. Frisbie, D. A. da Silva Filho, J.-L. Brédas, P. C. Ewbank and K. R. Mann, *Chem. Mater.*, 2004, **16**, 4436; (b) J. Zaumseil and H. Sirringhaus, *Chem. Rev.*, 2007, **107**, 1296; (c) A. Facchetti, *Mater. Today*, 2007, **10**, 28.
- Z. Bao, A. Lovinger and J. Brown, *J. Am. Chem. Soc.*, 1998, **120**, 207.
- M. L. Tang, J. H. Oh, A. D. Reichardt and Z. Bao, *J. Am. Chem. Soc.*, 2009, **131**, 3733.
- D. Schlettwein, D. Wöhrle, E. Karmann and U. Melville, *Chem. Mater.*, 1994, **6**, 3.
- X. Wang, Y. Zhang, X. Sun, Y. Bian, C. Ma and J. Jiang, *Inorg. Chem.*, 2007, **46**, 7136.
- (a) N. Sheng, Y. Zhang, H. Xu, M. Bao, X. Sun and J. Jiang, *Eur. J. Inorg. Chem.*, 2007, 3268; (b) N. Kobayashi and A. B. P. Lever, *J. Am. Chem. Soc.*, 1987, **109**, 7433.
- R. Li, D. Qi, J. Jiang and Y. Bian, *J. Porphyrins Phthalocyanines*, 2010, **14**, 421.
- G. J. Clarkson, N. B. McKeown and K. E. Treacher, *J. Chem. Soc., Perkin Trans. 1*, 1995, **14**, 1817.
- (a) N. Kobayashi, M. Togashi, T. Osa, K. Ishii, S. Yamauchi and H. Hino, *J. Am. Chem. Soc.*, 1996, **118**, 1073; (b) H. Miwa, K. Ishii and N. Kobayashi, *Chem.-Eur. J.*, 2003, **9**, 5123; (c) N. Kobayashi, S. Nakajima, H. Ogata and T. Fukuda, *Chem.-Eur. J.*, 2004, **10**, 6294; (d) X. Zhang, Y. Zhang and J. Jiang, *THEOCHEM*, 2004, **673**, 103.
- M. Kasha, H. R. Rawls and M. A. El-Bayoumi, *Pure Appl. Chem.*, 1965, **11**, 371.
- M. J. Cook and I. Chambrier, in *Porphyry Handbook, Phthalocyanines: Properties and Materials*, ed. K. M. Kadsh, K. M. Smith and R. Guillard, Elsevier Science, USA, 2003, vol. 17, pp. 37–127.
- (a) N. Nagata, S. Kugimiya and Y. Kobuke, *Chem. Commun.*, 2000, 1389; (b) Y. Kobuke and H. Miyaji, *J. Am. Chem. Soc.*, 1994, **116**, 4111.
- Y. Chen, L. Chen, G. Qi, H. Wu, Y. Zhang, L. Xue, P. P. Zhu, P. Ma and X. Li, *Langmuir*, 2010, **26**, 12473.
- (a) J. Jiang, M. Bao, L. Rintoul and D. P. Arnold, *Coord. Chem. Rev.*, 2006, **250**, 424; (b) M. Bao, R. Wang, L. Rintoul, D. P. Arnold and J. Jiang, *Vib. Spectrosc.*, 2006, **40**, 47; (c) W. Su, M. Bao and J. Jiang, *Vib. Spectrosc.*, 2005, **39**, 186; (d) M. Bao, Y. Bian, L. Rintoul, R. Wang, D. P. Arnold, C. Ma and J. Jiang, *Vib. Spectrosc.*, 2004, **34**, 283; (e) M. Bao, N. Pan, C. Ma, D. P. Arnold and J. Jiang, *Vib. Spectrosc.*, 2003, **32**, 175; (f) F. Lu, M. Bao, C. Ma, X. Zhang, D. P. Arnold and J. Jiang, *Spectrochim. Acta, Part A*, 2003, **59**, 3273; (g) J. Jiang, D. P. Arnold and H. Yu, *Polyhedron*, 1999, **18**, 2129.
- A. J. Bard, R. Parsons and J. Jordan, in *Standard Potentials in Aqueous Solution*, ed. A. J. Bard, J. Jordan and R. Parsons, Marcel Dekker, New York, 1985.
- SCE energy level is taken to be -4.44 eV below the vacuum level, for detail please see A. J. Bard and L. R. Faulkner, in *Electrochemical Methods-Fundamentals and Applications*, Wiley, New York, 1984.
- (a) Z. Wang, C. Kim, A. Facchetti and T. J. Marks, *J. Am. Chem. Soc.*, 2007, **129**, 13362; (b) B. A. Jones, A. Facchetti, M. R. Wasielewski and T. J. Marks, *J. Am. Chem. Soc.*, 2007, **129**, 15259.
- M. Kimura, T. Muto, H. Takimoto, K. Wada, K. Ohta, K. Hanabusa, H. Shirai and N. Kobayashi, *Langmuir*, 2000, **16**, 2078.
- F. Würthner, C. Thalacker, S. Diele and C. Tschierske, *Chem.-Eur. J.*, 2001, **7**, 2245.
- (a) J. Janczak and Y. M. Idemori, *Inorg. Chem.*, 2002, **41**, 5059; (b) A. S. Gardberg, S. Yang, B. M. Hoffman and J. A. Ibers, *Inorg. Chem.*, 2002, **41**, 1778.
- S. M. Sze, in *Physics of Semiconductor Devices*, John Wiley & Sons, New York, 1981.
- H. Z. Chen, M. M. Ling, X. Mo, M. M. Shi, M. Wang and Z. Bao, *Chem. Mater.*, 2007, **19**, 816.